Electrochemical Preparation and Characterization of Binuclear Palladium(I) Complexes Containing Aromatic Isocyanide and Chelating Diphosphine Ligands[1a]

Tomoaki Tanase, Kenji Kawahara, Hirokazu Ukaji, Kimiko Kobayashi,[1b] Hiroshi Yamazaki,[1b] and Yasuhiro Yamamoto*

Department of Chemistry, Faculty of Science, Toho University, Miyama, Funabashi, Chiba 274, Japan

Received February 2, 1993

A controlled-potential electrolysis was performed on mononuclear palladium(II) complexes containing aromatic isocyanide (RNC) and diphosphine (diphos) ligands, $[Pd(diphos)(RNC)_2](PF_6)_2$ (**3**) (R = 2,6-dimethylphenyl or 2,4,6-trimethylphenyl, diphos = *cis*-1,2-bis(diphenylphosphino)ethene (dppen), 1,2-bis(diphenylphosphino)ethane (dppe), 1,3-bis(diphenylphosphino)propane (dppp), or 1,4-bis(diphenylphosphino)butane (dppb)), which were derived from the reaction of $PdCl_2(COD)$ with diphos, RNC, and NH_4PF_6. A controlled-potential electrolysis of the complex **3** at a platinum-plate electrode consumed 1 F mol^{-1} in acetonitrile at −1.6 V (vs Cp_2Fe/Cp_2Fe^+), which gave a binuclear palladium(I) complex, $[Pd_2(diphos)_2(RNC)_2](PF_6)_2$ (**6**). They were characterized by IR, electronic, and ^1H and $^{31}P\{^1H\}$ NMR spectroscopies and X-ray crystallographic and EXAFS (extended X-ray absorption fine structure) analysis. The complex **6a** (R = 2,6-$Me_2C_6H_3$, diphos = dppen) crystallizes in the triclinic system, space group $P\bar{1}$, with a = 21.346(5) Å, b = 14.798(3) Å, c = 12.498(3) Å, α = 71.40(2)°, β = 103.14(2)°, γ = 82.92(2)°, and Z = 2 (R = 0.064 and R_w = 0.075 for 7052 independent reflections with $I > 2.5\sigma(I)$), and the complex **6e** (R = 2,4,6-$Me_3C_6H_2$, diphos = dppp) crystallizes in the monoclinic system, space group $P2_1/a$, with a = 25.963(11) Å, b = 19.247(4) Å, c = 14.963(9) Å, β = 101.49(4)°, and Z = 4 (R = 0.055 and R_w = 0.058 for 6885 independent reflections with $I > 1.5\sigma(I)$). The complexes **6** consist of two palladium atoms, each of them being coordinated by one isocyanide, one diphosphine, and the neighboring palladium atom in a square planar array. The diphosphines acted as chelating ligands. The lengths of the Pd–Pd bond fall within the range 2.59–2.62 Å, indicating that the Pd–Pd bond was hardly affected by the length of carbon chains of chelating diphosphines.

Introduction

Binuclear complexes having a metal–metal bond have been extensively studied because they promote some catalytic reactions and serve as models for heterogeneous catalysts.[2] In particular, much attention has been focused on the chemistry of binuclear palladium(I) and platinum(I) complexes bridged by bis(diphenylphosphino)methane (dppm), with regard to the ability to coordinate small molecules *via* additions across the metal–metal bond resulting in so-called "A-frame" complexes.[3,4] They were considered as plausible models for the catalytic intermediates generated on metal surfaces. Contrasted with a large number of reports concerning dppm bridged dimers, studies on the palladium and platinum complexes containing chelating diphosphines ($R_2P(CH_2)_nPR_2$, n = 2–4) were limited to the monomeric species, except for those on the coordinatively unsaturated binuclear platinum(0) complex with $^tBu_2P(CH_2)_3P^tBu_2$,[5] and the dipalladium(I) complex $[Pd_2(diphos)_2(MeNC)_2](PF_6)_2$ (diphos = $Ph_2P(CH_2)_nPPh_2$, n = 2–4).[6] The latter was isolated and characterized only by various spectroscopic methods.

Recently, we have studied the electrochemical preparations of bi-, tri-, and polynuclear palladium and platinum complexes of isocyanides (RNC). Electrochemical techniques have many advantages for preparations of low-valent transition-metal complexes by regulating the potential and the charge consumed. Controlled-potential electrolysis of $PtCl_2(RNC)_2$ at a mercury-pool electrode gave $Pt_2Cl_2(RNC)_4$, $Pt_3(RNC)_6$, or $[HgPt_6(RNC)_{12}]$,[7] and that of $[Pt(RNC)_4]^{2+}$ yielded $[Pt_2(RNC)_6]^{2+}$ or $[Pt_3(RNC)_8]^{2+}$,[8,9] depending on the coulometric conditions. By a similar procedure at a platinum-plate electrode, $PdCl_2(RNC)_2$ was readily reduced to the dimer $Pd_2Cl_2(RNC)_4$.[10] Recently, dppm was introduced to the electrochemical system as a supporting ligand for the metal–metal bonds. The electroreduction of $[Pt(dppm)(RNC)_2](PF_6)_2$ gave the dppm bridged dimer $[Pt_2(\mu\text{-dppm})_2(RNC)_2](PF_6)_2$ (**1**) and the trimetallic A-frame complex $[Pt_3(\mu\text{-dppm})_2(RNC)_4](PF_6)_2\cdot CH_2Cl_2$ (**2**).[8,9] The binuclear complex **1** reacted with $[HgPt_6(RNC)_{12}]$, which is a precursor of the 14-electron $Pt(RNC)_2$ fragment, to give the trimer **2** in a good yield through the insertion of the ML_2 fragment into the Pt–Pt σ-bond.[8]

In this study, instead of dppm, *cis*-1,2-bis(diphenylphosphino)ethene (dppen), 1,2-bis(diphenylphosphino)ethane (dppe), 1,3-bis(diphenylphosphino)propane (dppp), and 1,4-bis(diphenylphosphino)butane (dppb) were used to elucidate the effects of methylene chains of diphosphine ligands on the metal–metal-bonded structures. Here, we wish to report an electrochemical preparation of binuclear palladium(I) complexes containing aromatic isocyanide and chelating diphosphine ligands, which were characterized mainly by X-ray crystallographic and EXAFS (extended X-ray absorption fine structure) analyses.

Experimental Section

Acetonitrile was distilled over calcium hydride and $[^nBu_4N][ClO_4]$ was recrystallized from ethyl acetate prior to use. Other reagents were of the best commercial grade and were used without further purifications.

(1) (a) Electrochemical Studies of Organometallic Compounds. 9. Part 8: Yamamoto, Y.; Yamazaki, H. *Organometallics* **1983**, *12*, 933. (b) *RIKEN* (the Institute of Physical and Chemical Research), Wako, Saitama 351, Japan.
(2) Muetterties, E. L.; Rhodin, T. N.; Band, E.; Brucher, C. F.; Pretzer, W. R. *Chem. Rev.* **1979**, *79*, 91.
(3) Pudephatt, R. J. *Chem. Soc. Rev.* **1983**, *12*, 99.
(4) Balch, A. P. In *Homogeneous Catalysis with Metal Phosphine Complexes*; Pignolet, L. H., Ed.; Plenum Press: New York, 1983; p 167.
(5) Yoshida, T.; Yamagata, T.; Tulip, T. H.; Ibers, J. A.; Otsuka, S. *J. Am. Chem. Soc.* **1978**, *100*, 2063.
(6) Lindsay, C. H.; Benner, L. S.; Balch, A. L. *Inorg. Chem.* **1980**, *19*, 3503.
(7) (a) Yamamoto, Y.; Takahashi, K.; Matsuda, K.; Yamazaki, H. *J. Chem. Soc., Dalton Trans.* **1987**, 1833. (b) Yamamoto, Y.; Takahashi, K.; Yamazaki, H. *Chem. Lett.* **1985**, 201.
(8) Yamamoto, Y.; Takahashi, K.; Yamazaki, H. *J. Am. Chem. Soc.* **1986**, *108*, 2458.
(9) Yamamoto, Y.; Yamazaki, H. *Organometallics* **1993**, *12*, 933.
(10) Yamamoto, Y.; Takahashi, K.; Yamazaki, H. *Bull. Chem. Soc. Jpn.* **1987**, *60*, 2665.

0020-1669/93/1332-3682$04.00/0 © 1993 American Chemical Society

The isocyanides,[11] *cis*-1,2-bis(diphenylphosphino)ethene,[12]bis(di-*tert*-butylphosphino)ethane,[13] $PdCl_2(COD)$,[14] and $Pd_2Cl_2(RNC)_4$[15,16] were prepared by known methods. The following abbreviations are used: dppen, *cis*-1,2-bis(diphenylphosphino)ethene; dppe, 1,2-bis(diphenylphosphino)-ethane; dppp, 1,3-bis(diphenylphosphino)propane; dppb, 1,4-bis(diphenylphosphino)butane; dtbpe, 1,2-bis(di-*tert*-butylphosphino)ethane.

NMR spectroscopy was carried out on a JEOL GX-400 instrument at room temperature. ^1H NMR spectra were measured at 400 MHz in $CDCl_3$ using tetramethylsilane (TMS) as an internal reference, and $^{31}P\{^1H\}$ NMR spectra were measured at 160 MHz in CD_2Cl_2/CH_2Cl_2 mixed solvent using H_3PO_4 as an external reference. Infrared and electronic absorption spectra were recorded on Jasco A-100 and Ubest-30 spectrometers, respectively. Cyclic voltammetry and controlled-potential electrolyses were carried out using a HUSO 956B potentiostat and a HUSO 321 potential scanning unit. The electrolytic cell (H-type) consisted of a conventional three-electrode system, a platinum-plate electrode as a working electrode, a Pt wire as a counter electrode, and a $Ag/AgNO_3$ (0.1 M)–0.1 M $[^nBu_4N][ClO_4]$/MeCN system as a reference electrode. The counter electrode was separated by a glass filter. All potentials were calibrated relative to the Cp_2Fe/Cp_2Fe^+ (1.0 mM in MeCN) redox couple. $E_{1/2}(Cp_2Fe/Cp_2Fe^+)$ vs SCE was found at +0.42 V in acetonitrile.

Preparation of $[Pd(diphos)(RNC)_2](PF_6)_2$ (3) (diphos = dppen, dppe, dppp, and dppb). As a typical procedure, dppe (2.0 mmol), 2,6-$Me_2C_6H_3$-NC (4.0 mmol), and an excess of NH_4PF_6 (10.0 mmol) were successively added to a solution of CH_2Cl_2 (30 mL) and acetone (30 mL) containing 2.0 mmol of $PdCl_2(COD)$. The solution was stirred at room temperature for 2 h, and then the solvent was removed to dryness under reduced pressure. The residue was extracted with CH_2Cl_2 (ca. 60 mL), washed with H_2O (ca. 20 mL) and dried over Na_2SO_4. The resultant solution was concentrated to ca. 20 mL and an addition of diethyl ether gave pale yellow crystals of $[Pd(dppe)(2,6\text{-}Me_2C_6H_3NC)_2](PF_6)_2$ (**3b**). Yield: 82%. Anal. Calcd for $C_{44}H_{42}N_2PdP_4F_{12}$: C, 49.99; H, 4.00; N, 2.65. Found: C, 50.11; H, 4.05; N, 2.58. IR (Nujol): $\nu_{N\equiv C}$ 2215 cm^{-1}. UV–vis (CH_2Cl_2): λ_{max}(log ϵ) 300^{sh} (4.26), 232 (4.65) nm. ^1H NMR ($CDCl_3$): δ 2.08 (s, *o*-Me), 3.13 (m, CH_2), 6.9–8.0 (m, Ph). $[Pd(dppen)(2,6\text{-}Me_2C_6H_3NC)_2](PF_6)_2$ (**3a**). Yield: 79%. Anal. Calcd for $C_{44}H_{40}N_2PdP_4F_{12}$: C, 50.01; H, 3.82; N, 2.66. Found: C, 51.23; H, 3.50; N, 2.33. IR (Nujol): $\nu_{N\equiv C}$ 2196 cm^{-1}. UV–vis (CH_2Cl_2): λ_{max}(log ϵ) 245 (4.40) nm. ^1H NMR was not measured because of low solubility. $[Pd(dppe)(2,4,6\text{-}Me_3C_6H_2NC)_2](PF_6)_2$ (**3c**). Yield: 92%. Anal. Calcd for $C_{46}H_{46}N_2PdP_4F_{12}$: C, 50.91; H, 4.27; N, 2.58. Found: C, 50.54; H, 4.16; N, 2.44 (%). IR (Nujol): $\nu_{N\equiv C}$ 2209 cm^{-1}. UV–vis (CH_2Cl_2): λ_{max}(log ϵ) 255 (4.64) nm. ^1H NMR ($CDCl_3$): δ 2.03 (s, *o*-Me), 2.26 (s, *p*-Me), 3.03 (m, CH_2), 6.8–8.0 (m, Ph). $[Pd(dppp)(2,6\text{-}Me_2C_6H_3NC)_2](PF_6)_2$ (**3d**). Yield: 74%. Anal. Calcd for $C_{45}H_{44}N_2PdP_4F_{12}$: C, 50.46; H, 4.14; N, 2.62. Found: C, 50.52; H, 3.76; N, 2.44. IR (Nujol): $\nu_{N\equiv C}$ 2216 cm^{-1}. UV–vis (CH_2Cl_2): λ_{max}(log ϵ) 300^{sh} (4.15), 247 (4.54) nm. ^1H NMR ($CDCl_3$): δ 2.14 (s, *o*-Me), 1.85, 2.96 (br, CH_2), 6.9–7.8 (m, Ph). $[Pd(dppp)(2,4,6\text{-}Me_3C_6H_2NC)_2](PF_6)_2$ (**3e**). Yield: 82%. Anal. Calcd for $C_{47}H_{48}N_2PdP_4F_{12}$: C, 51.36; H, 4.40; N, 2.55. Found: C, 51.39; H, 4.21; N, 2.41. IR (Nujol): $\nu_{N\equiv C}$ 2212 cm^{-1}. UV–vis (CH_2Cl_2): λ_{max}(log ϵ) 256 (4.65) nm. ^1H NMR ($CDCl_3$): δ 2.05 (s, *o*-Me), 2.23 (s, *p*-Me) 2.38, 2.95 (m, CH_2), 6.7–7.8 (m, Ph). $[Pd(dppb)(2,6\text{-}Me_2C_6H_3NC)_2](PF_6)_2$ (**3f**). Yield: 79%. Anal. Calcd for $C_{46}H_{46}N_2PdP_4F_{12}$: C, 50.91; H, 4.27; N, 2.58. Found: C, 50.86; H, 4.28; N, 2.53. IR (Nujol): $\nu_{N\equiv C}$ 2209 cm^{-1}. UV–vis (CH_2Cl_2): λ_{max}(log ϵ) 275 (3.72) nm. ^1H NMR was not measured because of low solubility.

Preparation of $[Pd(dtbpe)(RNC)_2](PF_6)_2$ (4) and $[PdCl(dtbpe)(RNC)](PF_6)$ (5). All manipulations were carried out under a nitrogen atmosphere. To a solution of CH_2Cl_2 (60 mL) containing 3.0 mmol of $PdCl_2(COD)$ was added 3.0 mmol of dtbpe. The solution was stirred at room temperature for 2 h, and then the solvent was removed to dryness to give a white powder of $PdCl_2(dtbpe)$ quantitatively, which was washed with diethyl ether and dried in vacuo. Then 2.0 mmol of $PdCl_2(dtbpe)$ was dissolved in a mixed solvent of CH_2Cl_2 (30 mL) and acetone (30 mL), and 4.0 mmol of 2,6-$Me_2C_6H_3NC$ and an excess of NH_4PF_6 (10.0 mmol) were added to the solution. After 2 h, the solvent was removed to dryness and the residue was extracted with CH_2Cl_2 (ca. 60 mL). The organic layer was washed with H_2O (ca. 20 mL) and dried over Na_2SO_4. The CH_2Cl_2 solution was concentrated to about 20 mL and an addition of diethyl ether gave pale yellow crystals of $[Pd(dtbpe)(2,6\text{-}Me_2C_6H_3NC)_2](PF_6)_2$ (**4a**) in a yield of 42%. Anal. Calcd for $C_{36}H_{58}N_2PdP_4F_{12}$: C, 44.25; H, 5.98; N, 2.87. Found: C, 44.01; H, 6.17; N, 2.57. IR (Nujol): $\nu_{N\equiv C}$ 2204 cm^{-1}. UV–vis (CH_2Cl_2): λ_{max}(log ϵ) 243 (4.57), 234 (4.54) nm. ^1H NMR ($CDCl_3/CD_2Cl_2$): δ 1.57 (d, ^{t}Bu–P, J_{PH} = 15.6 Hz), 2.49 (s, *o*-Me), 2.66 (d, CH_2, J_{PH} = 16.1 Hz), 7.2∼7.4 (m, Ph). $[Pd(dtbpe)(2,4,6\text{-}Me_3C_6H_2NC)_2](PF_6)_2$ (**4b**). Yield: 55%. Anal. Calcd for $C_{38}H_{62}N_2PdP_4F_{12}$: C, 45.40; H, 6.22; N, 2.79. Found: C, 45.11; H, 6.37; N, 2.62. IR (Nujol): $\nu_{N\equiv C}$ 2200 cm^{-1}. UV–vis (CH_2Cl_2): λ_{max}(log ϵ) 248 (4.58) nm. ^1H NMR ($CDCl_3/CD_2Cl_2$): δ 1.56 (d, ^{t}Bu-P, J_{PH} = 15.1 Hz), 2.33 (s, *p*-Me), 2.43 (s, *o*-Me), 2.64 (d, CH_2, J_{PH} = 16.1 Hz), 7.00 (s, Ph).

In the preparation of **4b**, a careful crystallization of the mother liquid gave white crystals of $[PdCl(dtbpe)(2,4,6\text{-}Me_3C_6H_2NC)](PF_6)\cdot{}^1/_2CH_2Cl_2$ (**5b**). Yield: 17%. Anal. Calcd for $C_{28}H_{51}NPdClP_3F_6\cdot{}^1/_2CH_2Cl_2$: C, 43.17; H, 6.61; N, 1.77. Found: C, 43.20; H, 6.68; N, 1.74. IR (Nujol): $\nu_{N\equiv C}$ 2180 cm^{-1}. UV–vis (CH_2Cl_2): λ_{max}(log ϵ) 251 (4.57) nm. ^1H NMR ($CDCl_3/CD_2Cl_2$): δ 1.51 (d, ^{t}Bu–P, J_{PH} = 10.7 Hz), 1.55 (d, ^{t}Bu–P, J_{PH} = 10.5 Hz) 2.34 (s, *p*-Me), 2.46 (s, *o*-Me), 2.3∼2.6 (m, CH_2), 6.99 (s, Ph). Crystals of $[PdCl(dtbpe)(2,4,6\text{-}Me_3C_6H_2NC)](PF_6)\cdot H_2O$ suitable for X-ray analysis were obtained by recrystallization from a mixed solvent of wet THF and Et_2O.

Electrochemical Preparation of $[Pd_2(diphos)_2(RNC)_2](PF_6)_2$ (6) (diphos = dppen, dppe, dppp, and dppb). $[Pd(diphos)(RNC)_2](PF_6)_2$ (3) (0.2 mmol) was dissolved in 30 mL of 0.1 M acetonitrile solution of $NaClO_4$. The solution was deaerated by bubbling with nitrogen, and the reaction was monitored by cyclic voltammograms. After passage of the appropriate amount of charge (1 F mol^{-1}) at –1.6 V vs Cp_2Fe/Cp_2Fe^+ by using a platinum-plate working electrode, the solution was separated by decantation and solvent was removed under reduced pressure. The residue was extracted with CH_2Cl_2 (30 mL) and concentrated to ca. 10 mL, and an addition of diethyl ether gave yellow crystals of $[Pd_2(diphos)_2(RNC)_2](PF_6)_2$ (**6**). $[Pd_2(dppen)_2(2,6\text{-}Me_2C_6H_3NC)_2](PF_6)_2\cdot CH_2Cl_2$ (**6a**). Yield: 31%. Anal. Calcd for $C_{70}H_{62}N_2Pd_2P_6F_{12}\cdot CH_2Cl_2$: C, 51.91; H, 3.80; N, 1.71. Found: C, 52.18; H, 4.05; N, 1.75 (%). IR (Nujol): $\nu_{N\equiv C}$ 2140, 2154^{sh} cm^{-1}. UV–vis (CH_2Cl_2): λ_{max}(log ϵ) 434 (4.29), 338^{sh} (3.73), 268 (4.58) nm. ^1H NMR ($CDCl_3$): δ 1.82 (s, *o*-Me), 5.30 (s, CH_2Cl_2), 6.7–7.7 (m, CH=CH and Ph). $[Pd_2(dppe)_2(2,6\text{-}Me_2C_6H_3NC)_2](PF_6)_2\cdot{}^1/_2CH_2Cl_2$ (**6b**). Yield: 17%. Anal. Calcd for $C_{70}H_{66}N_2Pd_2P_6F_{12}\cdot{}^1/_2CH_2Cl_2$: C, 52.78; H, 4.21; N, 1.75. Found: C, 52.99; H, 4.33; N, 1.96. IR (Nujol): $\nu_{N\equiv C}$ 2145 cm^{-1}. UV–vis (CH_2Cl_2): λ_{max}(log ϵ) 424 (4.07), 342^{sh} (3.40), 272 (4.28) nm. ^1H NMR ($CDCl_3$): δ 2.17 (s, *o*-Me), 3.1∼3.3 (m, CH_2), 5.30 (s, CH_2Cl_2), 6.9–7.9 (m, Ph). $^{31}P\{^1H\}$ NMR (CD_2Cl_2/CH_2Cl_2): δ 38.73, 49.17 (br, $J_{PP'}$ = ∼0 Hz). $[Pd_2(dppe)_2(2,4,6\text{-}Me_3\text{-}C_6H_2NC)_2](PF_6)_2\cdot CH_2Cl_2$ (**6c**). Yield: 16%. Anal. Calcd for $C_{72}H_{70}N_2Pd_2P_6F_{12}\cdot CH_2Cl_2$: C, 52.35; H, 4.33; N, 1.67. Found: C, 52.59; H, 4.47; N, 1.45. IR (Nujol): $\nu_{N\equiv C}$ 2139 cm^{-1}. UV–vis (CH_2Cl_2): λ_{max}(log ϵ) 425 (4.20), 338 (3.65), 271 (4.44) nm. ^1H NMR ($CDCl_3$): δ 2.10 (s, *o*-Me), 2.37 (s, *p*-Me), 3.2∼3.3 (m, CH_2), 6.9–7.9 (m, Ph). $[Pd_2(dppp)_2(2,6\text{-}Me_2C_6H_3NC)_2](PF_6)_2$ (**6d**). Yield: 92%. Anal. Calcd for $C_{72}H_{70}N_2Pd_2P_6F_{12}$: C, 54.39; H, 4.44; N, 1.76. Found: C, 54.28; H, 4.38; N, 1.78. IR (Nujol): $\nu_{N\equiv C}$ 2146, 2162^{sh} cm^{-1}. UV–vis (CH_2Cl_2): ν_{max}(log ϵ) 426 (3.92), 271^{sh} (3.54), 233 (4.32) nm. ^1H NMR ($CDCl_3$): δ 1.93 (s, *o*-Me), 2.4∼3.2 (m, CH_2), 6.4–8.0 (m, Ph). $^{31}P\{^1H\}$ NMR (CD_2Cl_2/CH_2Cl_2): δ –15.09, 3.13 (d, $J_{PP'}$ = 20.2 Hz). $[Pd_2(dppp)_2(2,4,6\text{-}Me_3C_6H_2NC)_2](PF_6)_2$ (**6e**). Yield 27%. Anal. Calcd for $C_{74}H_{74}N_2Pd_2P_6F_{12}$: C, 54.93; H, 4.61; N, 1.73. Found: C, 54.75; H, 4.62; N, 1.80. IR (Nujol): $\nu_{N\equiv C}$ 2142, 2162^{sh} cm^{-1}. UV–vis (CH_2Cl_2): λ_{max}(log ϵ) 427 (4.25), 345 (3.77), 274 (4.49) nm. ^1H NMR ($CDCl_3$): δ 1.88 (s, *o*-Me), 2.38 (s, *p*-Me), 1.5∼3.1 (m, CH_2), 6.4–7.9 (m, Ph). $^{31}P\{^1H\}$ NMR (CD_2Cl_2/CH_2Cl_2): δ –15.24, 3.10 (d, $J_{PP'}$ = 19.6 Hz). $[Pd_2(dppb)_2(2,6\text{-}Me_2C_6H_3NC)_2](PF_6)_2$ (**6f**). Yield: 70%. Anal. Calcd for $C_{74}H_{74}N_2Pd_2P_6F_{12}$: C, 54.93; H, 4.61; N, 1.73. Found: C, 54.10; H, 4.50; N, 1.84. IR (Nujol): $\nu_{N\equiv C}$ 2151 cm^{-1}. UV–vis (CH_2Cl_2): λ_{max}(log ϵ) 421 (3.92), 343^{sh} (3.77), 265^{sh} (4.44) nm. ^1H NMR ($CDCl_3$): δ 1.71 (s, *o*-Me), 1.5∼3.1 (m, CH_2), 6.9–7.7 (m, Ph). $^{31}P\{^1H\}$ NMR (CD_2Cl_2/CH_2Cl_2): δ –4.15, 27.83 (d, $J_{PP'}$ = 18.5 Hz).

Photolysis of the Complex 6b. An acetonitrile solution containing 0.03 mM of **6b** and 0.15 mM of carbon tetrachloride was irradiated by a Rikokagaku UVL-100P 100-W high-pressure mercury lamp through a water IR filter. The photochemical reactions were monitored by electronic absorption spectra. $[PdCl(dppe)(2,6\text{-}Me_2C_6H_3NC)](PF_6)$ (**5a**)

(11) (a) Walborsky, H. M.; Niznik, G. E. *J. Org. Chem.* **1972**, *37*, 187. (b) Yamamoto, Y.; Aoki, K.; Yamazaki, H. *Inorg. Chem.* **1979**, *18*, 1681.
(12) Aguiar, A. M.; Daigle, D. *J. Am. Chem. Soc.* **1964**, *86*, 2299.
(13) Yamagata, T. Osaka University. Private communication.
(14) Drew, D.; Doyle, J. R. *Inorg. Synth.* **1972**, *13*, 52.
(15) (a) Otsuka, S.; Tatsuno, Y.; Ataka, K. *J. Am. Chem. Soc.* **1971**, *93*, 6705. (b) Boehm, J. R.; Balch, A. L. *Inorg. Chem.* **1977**, *16*, 778.
(16) Yamamoto, Y.; Yamazaki, H. *Bull. Chem. Soc. Jpn.* **1985**, *58*, 1843.

Table I. Crystallographic and Experimental Data for **5b**, **6a**, and **6e**

	5b	**6a**	**6e**
formula	$C_{28}H_{53}NPdClP_3F_6O$	$C_{71}H_{64}N_2Pd_2Cl_2P_6F_{12}$	$C_{74}H_{74}N_2Pd_2P_6F_{12}$
fw	768.50	1642.87	1618.08
cryst syst	monoclinic	triclinic	monoclinic
space group	$P2_1/c$ (No. 14)	$P\bar{1}$ (No. 2)	$P2_1/a$ (No. 14)
lattice const			
a, Å	11.139(1)	21.346(5)	25.963(11)
b, Å	15.548(2)	14.798(3)	19.247(4)
c, Å	21.237(3)	12.498(3)	14.963(9)
α, deg		71.40(2)	
β, deg	96.21(1)	103.14(2)	101.49(4)
γ, deg		82.92(2)	
V, Å^3	3656.5(9)	3561(1)	7327(6)
Z	4	2	4
T, °C	23	23	23
D_{calcd}, gcm^{-3}	1.396	1.533	1.467
μ, mm^{-1}	0.75	0.78	0.64
no. of unique data	1585 ($I > 3\sigma(I)$)	7052 ($I > 2.5\sigma(I)$)	6885 ($I > 1.5\sigma(I)$)
no. of param	370	1093	1162
R	0.070	0.064	0.055
R_w	0.057	0.075	0.058

[a] $R = \sum||F_o| - |F_c||/\sum|F_o|$. [b] $R_w = [\sum w(|F_o| - |F_c|)^2/\sum w|F_o|^2]^{1/2}$ ($w = 1/\sigma^2(F_o)$).

was prepared as follows. To a solution of dichloromethane containing 0.2 mmol of $PdCl_2$(dppe) were added 2,6-$Me_2C_6H_3NC$ (0.2 mmol) and NH_4PF_6 (0.2 mmol). The mixture was stirred for 1 h, and the solvent was removed under reduced pressure. The residue was extracted with CH_2Cl_2 (30 mL), concentrated to 10 mL, and an addition of Et_2O gave pale yellow crystals of **5a**, which were washed with Et_2O and dried in vacuo. Yield: 97%. Anal. Calcd for $C_{35}H_{33}NPdClP_3F_6$: C, 51.49; H, 4.07; N, 1.72. Found: C, 50.97; H, 3.81; N, 1.74. IR (Nujol): $\nu_{N\equiv C}$ 2201 cm^{-1}. UV–vis (CH_3CN): λ_{max}(log ϵ) 310 (3.90), 253 (4.47) nm.

Crystal Data and Intensity Measurements for [PdCl(dtbpe)(2,4,6-$Me_3C_6H_2NC$)]$(PF_6)\cdot H_2O$ (5b), [Pd_2(dppen)$_2$(2,6-$Me_2C_6H_3NC$)$_2$]$(PF_6)_2\cdot CH_2Cl_2$ (6a), and [Pd_2(dppp)$_2$(2,4,6-$Me_3C_6H_2NC$)$_2$]$(PF_6)_2$ (6e). Crystal data and experimental conditions for **5b**, **6a** and **6e** are listed in Table I. Colorless (**5b**) and yellow (**6a** and **6e**) crystals sealed into 0.7 mm o.d. glass-tube capillaries were used in the intensity data collection on a Rigaku four-circle automated diffractometer AFC5S (**5b**) and AFC4 (**6a**, **6e**) equipped with Mo Kα radiation. Three standard reflections were monitored every 100 reflections and showed no systematic decrease in intensity. A total of 3831 reflections (**5b**), 9124 reflections (**6a**), and 7550 reflections (**6e**) were measured and the intensities were corrected for Lorentz–polarization effects. Absorption corrections were applied.

Structure Solution and Refinement of 6a and 6e. The structure was solved by direct methods with MULTAN78.[20] The two palladium atoms were located in the initial E map, and subsequent Fourier syntheses gave the positions of other non-hydrogen atoms. The coordinates of all hydrogen atoms (except for those of the dichloromethane in **6a**) were determined by difference Fourier syntheses. The structure was refined with the block-diagonal least-squares techniques. Final refinement with anisotropic thermal parameters for non-hydrogen atoms and isotropic temperature factors for hydrogen atoms converged to $R = 0.064$ and $R_w = 0.075$, where $R = \sum||F_o| - |F_c||/\sum|F_o|$ and $R_w = [\sum\omega(|F_o| - |F_c|)^2/\sum w|F_o|^2]^{1/2}$ ($w = 1/\sigma^2(F_o)$), for **6a**, and $R = 0.055$ and $R_w = 0.058$ ($w = 1/\sigma^2(F_o)$) for **6e**. A final difference Fourier synthesis showed peaks at heights up to 1.6 e Å^{-3} around the Pd(1) atom (**6a**), and peaks at heights up to 0.60 e Å^{-3} around hexafluoro phosphate anion (**6e**). Atomic scattering factors and values of f' and f'' for Pd, Cl, P, F, N, and C were taken from refs 18 and 19. All calculations were carried out on a FACOM M-780 computer at the Computer Center of the Institute of Physical and Chemical Research with the Universal Crystallographic Computing Program System UNICS III.[20] Perspective views were drawn by using the program ORTEP.[21]

Structure Solution and Refinement of 5b. The structure was solved by direct methods with MITHRIL.[22] The palladium atom was located in the initial E map, and subsequent Fourier syntheses gave the positions of other non-hydrogen atoms. The coordinates of all hydrogen atoms except for those of the solvated molecule were calculated at the ideal positions with the C–H distance of 0.95 Å. The structure was refined with full-matrix least-squares techniques. Final refinement with anisotropic thermal parameters for non-hydrogen atoms (hydrogen atoms were not refined) converged to $R = 0.070$ and $R_w = 0.057$ ($w = 1/\sigma^2(F_o)$). A final difference Fourier synthesis showed peaks at heights up to 0.93 e Å^{-3} around the Pd atom. All calculations were carried out on a Digital VAX Station 3100 M38 with the TEXSAN-TEXRAY Program System.

X-ray Absorption Analysis. The X-ray absorption measurements were performed at the Photon Factory of the National Laboratory for High Energy Physics[23] on beam line 10B using synchrotron radiation (2.5 GeV, 340–300 mA). The experiments were done in the transmission mode on powdered samples using a Si(311) monochromator. Samples measured were **6a**, **6b**, **6d**, **6e**, and **6f**. The theoretical expression of the obtained $k^3\chi(k)$ for the case of single scattering is[24]

$$k^3\chi(k) = \sum_i (k^2N_i/r_i^2)S_iF_i(k)\exp(-2\sigma_i^2k^2)\sin(2kr_i + \Phi_i(k))$$

where r_i, N_i, S_i, $F_i(k)$, $\Phi_i(k)$, and σ_i represent the interatomic distance, the coordination number, the reducing factor, the backscattering amplitude, the phase shift, and the Debye–Waller factor, respectively, and k is the photoelectron wave vector defined as $k = [(2m/\hbar^2)(E - E_0)]^{1/2}$ ($E_0 = 24.348$ keV). The backscattering amplitude $F_i(k)$ and the phase shift $\Phi_i(k)$ functions employed were the empirical parameters derived from the analysis of **6e**[25] and the theoretical ones tabulated by Teo and Lee.[26,27] Three parameters, N_i, r_i, and σ_i, were varied in the nonlinear least-squares refined curve fitting. All calculations were performed on a *HITAC* S-800 computer at the Computer Center of the University of Tokyo with the systematic programs *EXAFS1*.[28]

Results and Discussion

Preparation of [Pd(diphos)(RNC)$_2$](PF$_6$)$_2$ (3, 4). The reaction of $PdCl_2$(COD) with diphosphines (diphos) and isocyanides (RNC) in the presence of an excess of NH_4PF_6 gave pale yellow complexes formulated as [Pd(diphos)(RNC)$_2$](PF$_6$)$_2$ (**3a**, diphos = dppen, R = 2,6-$Me_2C_6H_3$ (Xyl); **3b**, diphos = dppe, R = Xyl; **3c**, diphos = dppe, R = 2,4,6-$Me_3C_6H_2$ (Mes); **3d**, diphos = dppp, R = Xyl; **3e**, diphos = dppp, R = Mes; **3f**, diphos = dppb, R = Xyl) in good yields (74–92%). The IR spectra of **3** showed a peak at about 2200 cm^{-1}, corresponding to the terminal isocyanide groups ($\nu_{N\equiv C}$). Two IR absorptions corresponding to *sym*- and *asym*-stretching vibrations of the N≡C groups are expected in the compounds **3**, tentatively having a *cis*-geometry for RNC, but only one peak for the N≡C groups was observed, probably due to an accidental degeneracy. The ^{1}H NMR spectra indicated the presence of one kind of isocyanide and diphosphine ligands, and the electronic absorption spectra were similar to that of [Pd(RNC)$_4$](PF$_6$)$_2$,[10] indicating a square planar coordination geometry.

Similarly, the reaction of $PdCl_2$(dtbpe) with RNC and NH_4PF_6 gave [Pd(dtbpe)(RNC)$_2$](PF$_6$)$_2$ (**4a**, R = Xyl; **4b**, R = Mes) in moderate yields. The IR spectra of **4** also showed a peak for the N≡C stretching at 2200–2204 cm^{-1}. In the ^{1}H NMR spectra, only one resonance for ^{t}Bu groups was observed at $\delta \sim 1.56$ as a doublet ($J_{PH} \sim 15$ Hz) and one peak for the *o*-methyl groups of isocyanides at $\delta \sim 2.45$ as a singlet. In the preparation of **4b**, [PdCl(dtbpe)(MesNC)](PF$_6$)$\cdot^1/_2CH_2Cl_2$ (**5b**) was obtained as

(17) Main, P.; Lessinger, L.; Woolfson, M. M.; Germain, G.; Declerq, J. P. MULTAN78. Universities of York, England, and Louvain, Belgium, 1978.
(18) Cromer, D. T.; Waber, J. T. *International Tables for X-ray Crystallography*; Kynoch Press: Birmingham, England, 1974; Vol IV.
(19) Cromer, D. T. *Acta Crystallogr.* **1965**, *18*, 17.
(20) Sakurai, T.; Kobayashi, K. *Rikagaku Kenkyusho Hokoku* **1979**, *55*, 69.
(21) Johnson, C. K. ORTEP-II, a FORTRAN Thermal Ellipsoid Plot Program. Oak Ridge National Laboratory, Oak Ridge, TN, 1976.
(22) Gilmore, G. J. *J. Appl. Crystallogr.* **1984**, *17*, 42.
(23) *Photon Factory Activity Report*; National Laboratory for High Energy Physics: Ibaraki, Japan, 1986; No. 3.
(24) Sayers, D. E.; Stern, E. A.; Lytle, F. W. *Phys. Rev. Lett.* **1971**, *27*, 1204.
(25) Cramer, S. P.; Hodgson, K. O.; Gillum, W. O.; Mortenson, L. E. *J. Am. Chem. Soc.* **1978**, *100*, 3398.
(26) Teo, B. K.; Lee, P. A.; Simons, A. L.; Eisenberger, P.; Kincaid, B. M. *J. Am. Chem. Soc.* **1977**, *99*, 3854.
(27) Teo, B. K.; Lee, P. A. *J. Am. Chem. Soc.* **1979**, *101*, 2815.
(28) Kosugi, N.; Kuroda, H. *Program EXAFS1*; Research Center for Spectrochemistry, the University of Tokyo: Tokyo, Japan, 1985.

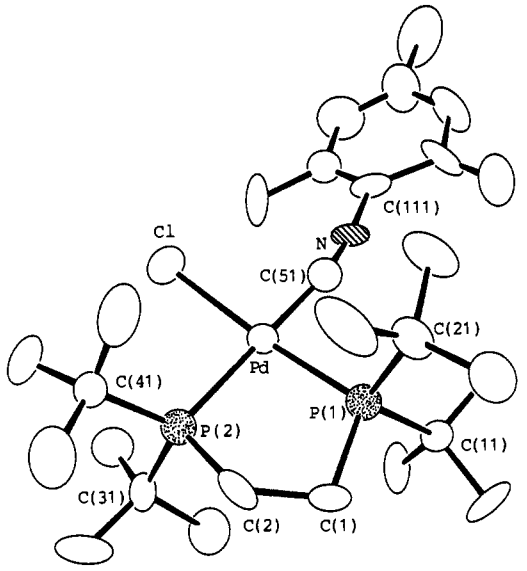

Figure 1. Perspective drawing of the complex cation of **5b**, $[PdCl(dtbpe)(XylNC)]^+$.

Table II. Selected Bond Distances (Å) and Angles (deg) of **5b**[a]

Bond Distances			
Pd–Cl	2.342(6)	Pd–P(1)	2.274(7)
Pd–P(2)	2.325(7)	Pd–C(51)	1.99(3)
P(1)–C(1)	1.83(2)	P(1)–C(11)	1.87(2)
P(1)–C(21)	1.88(2)	P(2)–C(2)	1.81(2)
P(2)–C(31)	1.90(3)	P(2)–C(41)	1.88(2)
N–C(51)	1.17(3)	N–C(111)	1.37(3)
C(1)–C(2)	1.59(3)		
Bond Angles			
Cl–Pd–P(1)	171.9(3)	Cl–Pd–P(2)	93.4(2)
Cl–Pd–C(51)	84.1(7)	P(1)–Pd–P(2)	87.5(2)
P(1)–Pd–C(51)	96.1(7)	P(2)–Pd–C(51)	171.8(7)
C(51)–N–C(111)	173(3)	Pd–C(51)–N	171(2)

[a] Estimated standard deviations in parentheses.

a minor product. The complex **5b** was readily converted to **4b** by treatment with an equimolar amount of MesNC and NH_4PF_6. Analytical and IR and ^1H NMR spectral data indicated that the complex **5b** has a structure similar to that of **4**, in which one isocyanide ligand is replaced by a chlorine atom. The structure was confirmed by an X-ray crystallographic analysis. A perspective drawing of the complex cation of **5b**, along with the atom-labeling scheme, is shown in Figure 1, and some selected bond lengths and angles are listed in Table II. The central palladium atom is coordinated by a bidentate dtbpe, an isocyanide, and a chlorine atom in a square planar array; the distances of Pd–Cl (2.342(6) Å), Pd–P (2.274(4), 2.325(7) Å) and Pd–C (1.99(3) Å) fall within the normal ranges. The five-membered chelate ring comprised of dtbpe adopts a *gauche* conformation, and the bite angle of P(1)–Pd–P(2) is 87.5(2)°. The *cis* angle of Cl(1)–Pd–C(51) (84.1(7)°) is smaller than the ideal value of 90°, presumably due to the steric repulsion between the bulky ^{t}Bu groups of dtbpe and the isocyanide ligand (P(1)–Pd–C(51) 96.1(7)°).

Cyclic voltammograms of the compounds **3** in acetonitrile showed two irreversible reduction waves at −1.0 to −1.1 V (E_1) and −1.1 to −1.4 V (E_2) (vs Cp_2Fe/Cp_2Fe^+) (Table III and Figure 2). By analogy with that of $[Pd(RNC)_4](PF_6)_2$, they were assignable to a two-step one-electron reduction, Pd(II) → Pd(I) and Pd(I) → Pd(0), respectively.[9,10] The reduction potentials of **3a** (diphos = dppen; R = Xyl) were higher than those of the other complexes **3b–3f** (by ~0.1 V for E_1 and ~0.2 V for E_2), reflecting the lower basicity of dppen than the diphosphines having methylene chains. The dtbpe compound **4** also showed two irreversible reduction waves and the potential of the second wave

Table III. Reduction Peak Potentials of $[Pd(diphos)(RNC)_2]^{2+}$ (**3** and **4**)[a]

complex	E_1, V[b]	E_2, V[b]
$[Pd(dppen)(XylNC)_2]^{2+}$ (**3a**)	−1.00	−1.16
$[Pd(dppe)(XylNC)_2]^{2+}$ (**3b**)	−1.12	−1.35
$[Pd(dppe)(MesNC)_2]^{2+}$ (**3c**)	−1.13	−1.39
$[Pd(dppp)(XylNC)_2]^{2+}$ (**3d**)	−1.08	−1.35
$[Pd(dppp)(MesNC)_2]^{2+}$ (**3e**)	−1.11	−1.38
$[Pd(dppb)(XylNC)_2]^{2+}$ (**3f**)	−1.10	−1.35
$[Pd(dtbpe)(XylNC)_2]^{2+}$ (**4a**)	−1.12	−1.57
$[Pd(dtbpe)(MesNC)_2]^{2+}$ (**4b**)	−1.22	−1.57

[a] Cyclic voltammograms were measured on 0.5–1.0 mM solutions of the complexes in acetonitrile containing 0.1 M $[^nBu_4N][ClO_4]$ by means of a platinum working electrode with a scaning rate of 200 mV/s. [b] Referenced to the $E_{1/2}$ of the redox coupling Cp_2Fe/Cp_2Fe^+ (1.0 mM in CH_3CN).

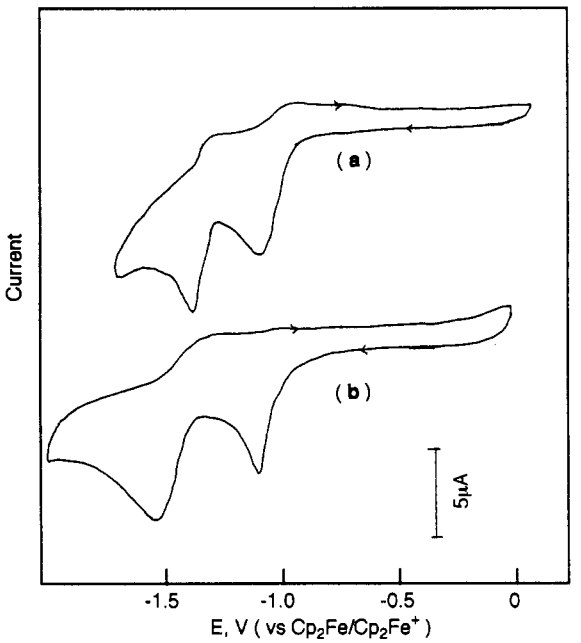

Figure 2. Cyclic voltammograms of (a) $[Pd(dppe)(XylNC)_2](PF_6)_2$ (**3b**) and (b) $[Pd(dtbpe)(XylNC)_2](PF_6)_2$ (**4a**) in acetonitrile containing 0.1 M $[^nBu_4N][ClO_4]$. The working electrode is Pt and the scanning rate is 200 mV/s.

(E_2) is lower by ca. 0.2 V than those for the dppe complexes **3b** and **3c**, due to the high electron-donating ability of dtbpe.

Electrochemical Preparation of $[Pd_2(diphos)_2(RNC)_2](PF_6)_2$ (6). The controlled potential electroreduction of **3** in acetonitrile at a platinum-plate electrode was carried out at ca. −1.6 V (lower potential than E_2). After the passage of ca. 1 F mol^{-1} of **3**, the yellow complexes, formulated as $[Pd_2(diphos)_2(RNC)_2](PF_6)_2$ (**6**), were obtained in yields of 15–92% (**6a**, diphos = dppen, R = Xyl; **6b**, diphos = dppe, R = Xyl; **6c**, diphos = dppe, R = Mes; **6d**, diphos = dppp, R = Xyl; **6e**, diphos = dppp, R = Mes; **6f**, diphos = dppb, R = Xyl). When the electrolysis was carried out at about −1.2 V (between E_1 and E_2), the yields of **6** decreased and the starting complexes were recovered. The electrochemical reaction at ca. −1.6 V was considered to involve an initial two-electron reduction of Pd(II) to Pd(0) and a subsequent conproportionation process, Pd(0) + Pd(II) → 2 Pd(I).

The IR spectra of the complexes **6** showed a sharp peak around 2140 cm^{-1}, corresponding to the terminal isocyanide groups, some of which were accompanied by a shoulder peak at the high-energy side. The $\nu_{N\equiv C}$ frequencies shifted to lower energy by ca. 70 cm^{-1} than those of **3**, indicating that the divalent palladium center was reduced to a monovalent species. In the UV–vis spectra, an absorption band was observed at about 420~440 nm, assigned to the σ–σ^* transition by analogy with $[Pd_2(MeNC)_6]^{2+}$ (**8**)[29–31] and $Pd_2Cl_2(^tBuNC)_4$ (**9**),[16] and further on the basis of our

photochemical reaction of **6b** (*vide infra*). The ^1H NMR spectra indicated the presence of one kind of isocyanide ligand, and the $^{31}P\{^1H\}$ NMR spectra showed two doublet resonances in the region of −15 to +50 ppm relative to H_3PO_4 with small coupling constants of $J_{PP'}$ = 0–20 Hz, indicating a structure in which each end of the diphosphine ligand is in a chemically distinct environment.[6] The small coupling constants ($J_{PP'}$) are indicative of a *cis* orientation of the two dissimilar phosphorus atoms. These spectral data suggested that the complex **6** has a binuclear structure with a Pd(I)–Pd(I) σ-bond, in which the diphosphine ligands chelate to a Pd atom (depicted as A), and do not act as bridging ligands between two Pd atoms as does dppm (as B). The B type dimer

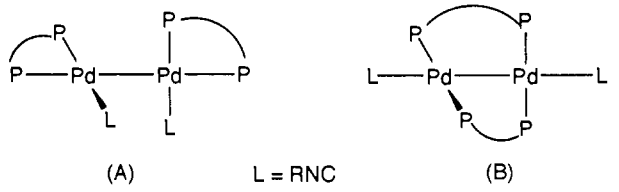

with bridging diphosphines was not obtained in the electrochemical reactions, probably due to instability of large-membered metal-containing macrocyclic conformations. The complexes **6** could also be prepared by the substitution reaction of $Pd_2Cl_2(RNC)_4$ (**7**) (R = Xyl, Mes) with 2 equiv of diphosphines (dppen, dppe, dppp, and dppb) in the presence of an excess amount of NH_4PF_6 in good yields. Similar complexes were already prepared by the reaction of $[Pd_2(MeNC)_6]^{2+}$ (**8**) with diphosphines.[6]

The bonding in the $Pd_2P_4C_2$ system of **6** can be understood from the combination of two T-shaped PdP_2C fragments (15 valence electrons) to form σ and σ^* molecular orbitals; the former is the HOMO and the latter is the LUMO from the extended Huckel MO calculations. From the bonding system, the lowest energy band around 425 nm of **6** was assignable to a σ-σ^* transition, and there was no dependence of λ_{max} on solvent (424 nm in CH_2Cl_2, 425 nm in CH_3CN, and 425 nm in $(CH_3)_2CO$ for **6b**). The energies of the band maxima were considerably shifted to the lower energy side compared with $[Pd_2(MeNC)_6](PF_6)_2$ (**8**) (307 nm in CH_2Cl_2)[31] and $PdCl_2(^tBuNC)_4$ (**9**) (307 nm in CH_2Cl_2).[16] In order to confirm the assignment, a photochemical reaction was carried out in the **6b**–CCl_4 system. It is known that the photoexcitation of the $[Pd^I_2L_6]^{2+}$ complex affords the σ–σ^* excited states which homolytically cleave to two d^9 $Pd^IL_3^{\bullet+}$ radical cations, and they easily abstract a halogen atom from CX_4 to give $[Pd^{II}XL_3]^+$ species.[31] Photolysis of a mixture of **6b** (0.03 mM) and CCl_4 (0.15 mM) in CH_3CN was monitored by UV–vis absorption spectroscopy as shown in Figure 3. The intense band at 425 nm decreased during the photolysis and finally the spectrum was in accordance with that of $[PdCl(dppe)(XylNC)](PF_6)$ (**5a**), indicating a cleavage of the metal–metal bond. Thus, the absorption around 425 nm is ascribable to the σ–σ^* transition.

The controlled-potential electrolysis of $[Pd(dtbpe)(RNC)_2](PF_6)_2$ (**4**) at −1.8 V consumed 1 F mol^{-1} of **4**, but no dimeric complex involving Pd–Pd bond was isolated from the resultant solution. The chemical reaction of $[Pd_2(RNC)_6](PF_6)_2$ with 2 equiv of dtbpe also gave the mononuclear compound **4** without forming a palladium(I) dimer. This failure implied the highly instable nature of the Pd–Pd bond in $[Pd_2(dtbpe)_2(RNC)_2]^{2+}$, presumably due to the elongation of the Pd–Pd bond by the steric repulsion between adjacent bulky dtbpe ligands.

Structure of $[Pd_2(dppe)_2(2,4,6\text{-}Me_3C_6H_2NC)_2](PF_6)_2$ (6e) and $[Pd_2(dppen)_2(2,6\text{-}Me_2C_6H_3NC)_2](PF_6)_2\cdot CH_2Cl_2$ (6a). The asymmetric unit of **6e** contains the discrete complex cation and two

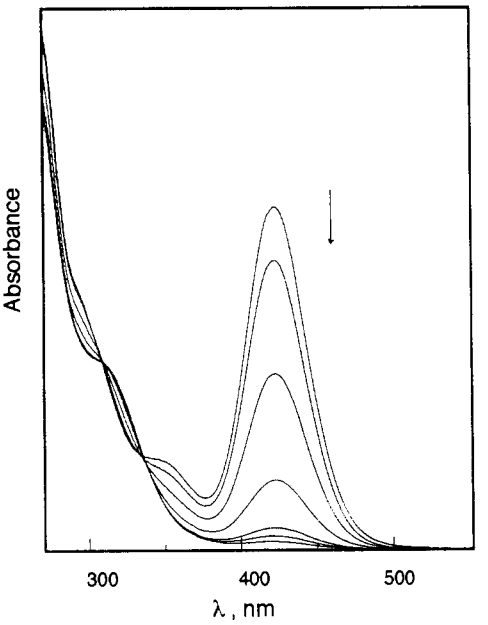

Figure 3. Change of electronic spectrum of $[Pd_2(dppe)_2(XylNC)_2]^{2+}$ (**6b**) during the photolysis. Spectra were recorded every 5 min.

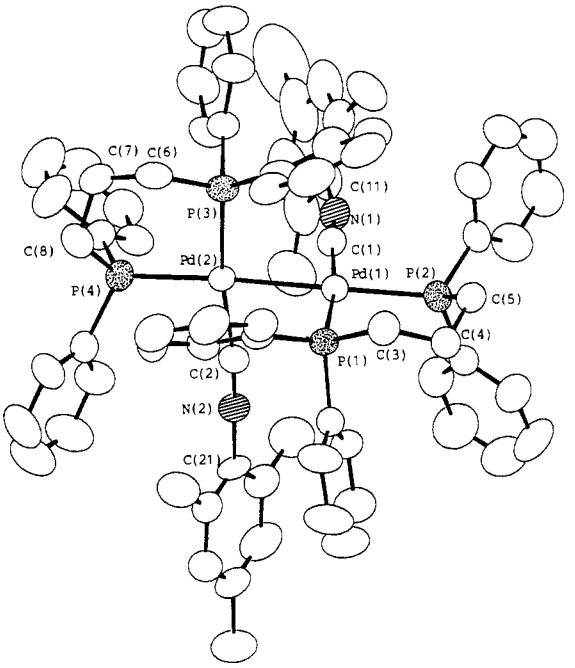

Figure 4. Perspective drawing of the complex cation of **6e**, $[Pd_2(dppp)_2(MesNC)_2]^{2+}$.

hexafluorophosphate anions. There is no unusual contact between these subunits. A perspective drawing of the complex cation of **6e** with the atomic numbering scheme is given in Figure 4. Some selected bond distances and angles are listed in Table IV. The complex cation consists of two palladium atoms joined by a palladium–palladium σ-bond. The cation has no crystallographically imposed symmetry, but its ideal symmetry is C_2. Each palladium atom is coordinated by two phosphorus atoms of bidentate dppp ligand, one carbon atom of isocyanide molecule, and another palladium atom in a nearly planar array. The dihedral angle between the two $[PdP_2C]$ coordination planes is 86°, nearly perpendicular as observed in **8** (86.4°), **9** (82.7°), and **10** (85.3°). It should be noted that a dihedral angle of 90° is ideal for minimizing the repulsion between the ligands and an angle of 45° is ideal for minimizing repulsive overlap of the out-of-plane metal dπ orbitals on adjacent metal centers.[32] In the nonbridged

(29) Doonan, D. J.; Balch, A. L.; Goldberg, S. Z.; Eisenberg, R.; Miller, J. S. *J. Am. Chem. Soc.* **1975**, *97*, 1961.
(30) Goldberg, S. Z.; Eisenberg, R. *Inorg. Chem.* **1976**, *15*, 535.
(31) Reinking, M. K.; Kullberg, M. L.; Cutler, A. R.; Kubiak, C. P. *J. Am. Chem. Soc.* **1985**, *107*, 3517.

Table IV. Selected Bond Distances (Å) and Angles (deg) of **6e**[a]

Bond Distances			
Pd(1)–Pd(2)	2.617(2)		
Pd(1)–P(1)	2.334(2)	Pd(1)–P(2)	2.345(3)
Pd(2)–P(3)	2.301(2)	Pd(2)–P(4)	2.374(3)
Pd(1)–C(1)	1.962(8)	Pd(2)–C(2)	1.973(8)
P(1)–C(3)	1.82(1)	P(2)–C(5)	1.83(1)
P(3)–C(6)	1.83(1)	P(4)–C(8)	1.82(1)
N(1)–C(1)	1.15(1)	N(1)–C(11)	1.41(1)
N(2)–C(2)	1.16(1)	N(2)–C(21)	1.42(1)
C(3)–C(4)	1.54(1)	C(4)–C(5)	1.52(1)
C(6)–C(7)	1.54(1)	C(7)–C(8)	1.51(1)
Bond Angles			
Pd(2)–Pd(1)–P(1)	96.76(7)	Pd(2)–Pd(1)–P(2)	168.05(7)
Pd(2)–Pd(1)–C(1)	75.1(3)	P(1)–Pd(1)–P(2)	93.76(9)
P(1)–Pd(1)–C(1)	171.6(3)	P(2)–Pd(1)–C(1)	94.6(3)
Pd(1)–Pd(2)–P(3)	88.58(8)	Pd(1)–Pd(2)–P(4)	176.51(6)
Pd(1)–Pd(2)–C(2)	82.2(3)	P(3)–Pd(2)–P(4)	94.67(9)
P(3)–Pd(2)–C(2)	169.7(3)	P(4)–Pd(2)–C(2)	94.5(3)
Pd(1)–P(1)–C(3)	112.1(3)	Pd(1)–P(2)–C(5)	114.8(3)
Pd(2)–P(3)–C(6)	111.6(3)	Pd(2)–P(4)–C(8)	111.3(4)
C(1)–N(1)–C(11)	168.8(9)	C(2)–N(2)–C(21)	178.8(9)
Pd(1)–C(1)–N(1)	174.5(8)	Pd(2)–C(2)–N(2)	171.7(8)
P(1)–C(3)–C(4)	115.2(6)	P(2)–C(5)–C(4)	114.8(7)
P(3)–C(6)–C(7)	116.0(6)	P(4)–C(8)–C(7)	115.0(7)
C(3)–C(4)–C(5)	115.2(7)	C(6)–C(7)–C(8)	115.0(7)

[a] Estimated standard deviations in parentheses.

dimer **6e**, the steric factor seems to be mainly responsible for the observed structure.

The Pd–Pd bond is not supported by any bridging ligands and the length of 2.617(2) Å is significantly longer than those of unbridged palladium(I) dimers of isocyanides, $Pd_2Cl_2(^tBuNC)_4$ (**9**) (2.532(2) Å),[16] $Pd_2I_2(MeNC)_4$ (**10**) (2.533(1) Å),[33] and $[Pd_2(MeNC)_6](PF_6)_2$ (**8**) (2.531(9) Å),[29,30,34] and shorter than those found in dppm bridged dimers, $Pd_2Cl_2(\mu\text{-dppm})_2$ (2.699(2) Å)[35] and $Pd_2Cl(SnCl_3)(\mu\text{-dppm})_2$ (2.644 Å).[36] The bond lengths between the axial phosphorus and palladium atoms (Pd(1)–P(2) 2.345(3) Å, Pd(2)–P(4) 2.374(3) Å) are slightly longer than those between the equatorial P and Pd atoms (Pd(1)–P(1) 2.334(2) Å, Pd(2)–P(3) 2.301(2) Å), arising from the high *trans* effect of the Pd–Pd σ-bond as observed in **9** and **10**. The axial P atoms are almost colinear with the Pd–Pd bond. The average Pd–Pd–P_{ax} angle is 172.3°. The six-membered chelate rings adopt the stable chair conformation and the average bite angle is 94.2°. Recently, a novel "side-on" Pd–P interaction was reported on the palladium(I) dimer of dppp, $[Pd_2(dppp)_2](CF_3SO_3)_2$, where a short distance between the ipso carbon of a phenyl group at the equatorial phosphine and the adjacent palladium atom was observed at 2.39(2) Å.[37] In the compound **6e**, there is no short contact (<3.3 Å) between the phenyl rings on the equatorial phosphorus atom and the neighboring palladium atom.

The average of the Pd–C–N angles is 173.1°, and that of the C–N–C angles is 173.8°, falling within the usual range for terminal isocyanides. The isocyanide ligands are considerably bent toward the Pd–Pd bond. The average Pd–Pd–C angle is 78.7°, which is smaller than those found in the dimers **8** (average 85.0°), **9** (83.0°), and **10** (average 84.7°), and is comparable to that in the palladium trimer $[Pd_3(PPh_3)_2(MeNC)_6]^{2+}$ (**11**) (average 80.0°).[38]

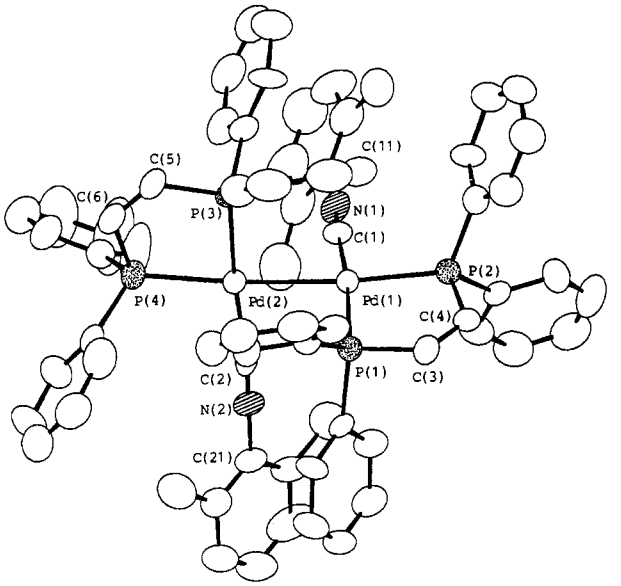

Figure 5. Perspective drawing of the complex cation of **6a**, $[Pd_2(dppen)_2(XylNC)_2]^{2+}$.

Table V. Selected Bond Distances (Å) and Angles (deg) of **6a**[a]

Bond Distances			
Pd(1)–Pd(2)	2.602(1)		
Pd(1)–P(1)	2.298(3)	Pd(1)–P(2)	2.320(3)
Pd(2)–P(3)	2.301(3)	Pd(2)–P(4)	2.326(3)
Pd(1)–C(1)	1.96(1)	Pd(2)–C(2)	1.97(1)
P(1)–C(3)	1.84(1)	P(2)–C(4)	1.81(1)
P(3)–C(5)	1.82(1)	P(4)–C(6)	1.80(1)
N(1)–C(1)	1.16(2)	N(1)–C(11)	1.42(2)
N(2)–C(2)	1.17(2)	N(2)–C(21)	1.41(2)
C(3)–C(4)	1.29(2)	C(5)–C(6)	1.32(2)
Bond Angles			
Pd(2)–Pd(1)–P(1)	95.27(8)	Pd(2)–Pd(1)–P(2)	174.39(8)
Pd(2)–Pd(1)–C(1)	78.8(3)	P(1)–Pd(1)–P(2)	86.1(1)
P(1)–Pd(1)–C(1)	170.7(4)	P(2)–Pd(1)–C(1)	100.6(4)
Pd(1)–Pd(2)–P(3)	89.71(9)	Pd(1)–Pd(2)–P(4)	174.70(9)
Pd(1)–Pd(2)–C(2)	84.8(3)	P(3)–Pd(2)–P(4)	85.0(1)
P(3)–Pd(2)–C(2)	173.8(3)	P(4)–Pd(2)–C(2)	100.5(3)
Pd(1)–P(1)–C(3)	105.7(4)	Pd(1)–P(2)–C(4)	106.8(4)
Pd(2)–P(3)–C(5)	106.6(4)	Pd(2)–P(4)–C(6)	106.4(4)
C(1)–N(1)–C(11)	174(1)	C(2)–N(2)–C(21)	177(1)
Pd(1)–C(1)–N(1)	174.3(8)	Pd(2)–C(2)–N(2)	173.8(10)
P(1)–C(3)–C(4)	121.3(9)	P(2)–C(4)–C(3)	120.0(8)
P(3)–C(5)–C(6)	119.8(8)	P(4)–C(6)–C(5)	120.0(8)

[a] Estimated standard deviations in parentheses.

The largest inward bend of Pd(2)–Pd(1)–C(1) (75.1(3)°) brings the Pd(2)···C(1) distance to within the sum of the van der Waals radii of the two atoms (2.87(3) Å). This large inward bend of the equatorial isocyanides is largely attributable to the steric bulk of dppp ligands. It is in part caused by an electronic effect arising from interaction between the filled d orbitals of the palladium with the empty π* orbitals of the isocyanide ligands on the adjacent metal. An explanation of this bending has been already reported.[30]

The asymmetric unit of **6a** contains the complex cation, two hexafluorophosphate anions, and one dichloromethane molecule. There is no unusual contact between them. A perspective drawing of the complex cation of **6a** with the atomic numbering scheme is given in Figure 5. Some selected bond distances and angles are listed in Table V. The complex cation of **6a** has a binuclear structure similar to that observed in **6e**. The dihedral angle between the two $[PdP_2C]$ planes is 78.0(1)°. The length of the Pd–Pd bond is 2.602(1) Å, slightly shorter than found in **6e**. The Pd–P_{ax} bond lengths (Pd(1)–P(2) 2.320(3) Å, Pd(2)–P(4) 2.326(3) Å) are longer by ~0.02 Å than the Pd–P_{eq} distances (Pd(1)–P(1) 2.298(3) Å, Pd(2)–P(3) 2.301(3) Å). The five-

(32) Kullberg, M. L.; Lemke, F. R.; Powell, D. R.; Kubiak, C. P. *Inorg. Chem.* **1985**, *24*, 3589.
(33) Rutherford, N. M.; Olmstead, M. M.; Balch, A. L. *Inorg. Chem.* **1984**, *23*, 2833.
(34) Miller, T. D.; Clair, M. A. St.; Reinking, M. K.; Kubiak, C. P. *Organometallics* **1983**, *2*, 767.
(35) Holloway, R. G.; Penfold, B. R.; Colton, R.; McCormick, M. J. *J. Chem. Soc., Chem. Commun.* **1976**, 485.
(36) Olmstead, M. M.; Nenner, L. S.; Hope, H.; Balch, A. L. *Inorg. Chim. Acta* **1979**, *32*, 193.
(37) Budzelaar, P. H. M.; van Leeuwen, P. W. N. M.; Roobeak, C. F. *Organometallics* **1992**, *11*, 23.
(38) Balch, A. L.; Boehm, J. R.; Hope, H.; Olmstead, M. M. *J. Am. Chem. Soc.* **1976**, *98*, 7431.

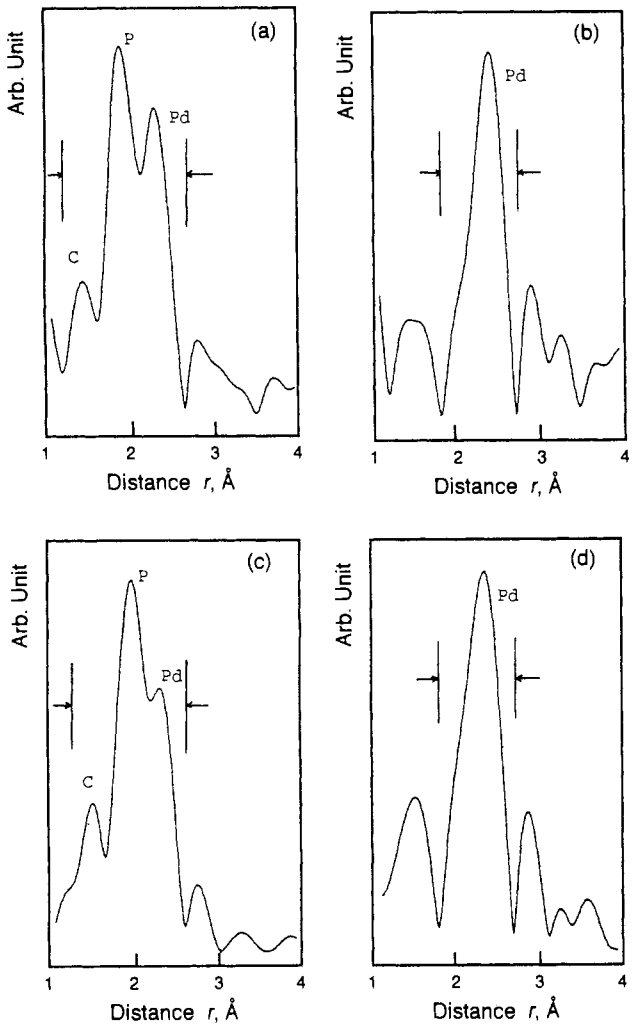

Figure 6. (a) Fourier transform of $k^3\chi_{obsd}(k)$ for **6e**. (b) Difference Fourier transform of $[k^3\chi_{obsd}(k) - (k^3\chi_C(k) + k^3\chi_P(k))]$ for **6e**. (c) Fourier transform of $k^3\chi_{obsd}(k)$ for **6a**. (d) Difference Fourier transform of $[k^3\chi_{obsd}(k) - (k^3\chi_C(k) + k^3\chi_P(k))]$ for **6a**.

membered chelate rings involving dppen ligands adopt the envelop form (^{Pd}E) and the average bite angle is 85.6°. It is assumed that the small chelation angle of **6a** (compared with **6e**) decreases steric repulsions between the two PdP_2C units, resulting in the slightly shortened Pd–Pd bond distance in **6a**. The terminal isocyanides are linearly coordinated to the Pd atom (average Pd–C–N angle is 174° and average C–N–C angle is 175°), and the inward bend of isocyanides is also observed; the average Pd–Pd–C angle of 81.8° is larger than that found in **6e**. The closest contact between the Pd atom and the terminal carbon atom of RNC on the adjacent Pd atom is 2.94(3) Å (Pd(1)···C(2)).

EXAFS Analyses. In order to examine the length of palladium–palladium bond of other dipalladium complexes, EXAFS (extended X-ray absorption fine structure) analyses were performed on **6a**, **6b**, **6d**, **6e**, and **6f**.

The Fourier transform of **6e** showed three peaks in the range 1.1–2.7 Å (before phase-shift correction) (Figure 6a), the small peak at ca. 1.6 Å assignable to the backscattering contribution

Table VI. Stuctural Parameters of Pd–Pd Bonds Derived from EXAFS Analyses

complex	r(Pd–Pd), Å[a]	N[b]	σ	R, %[c]
$[Pd_2(dppp)_2(MesNC)_2]^{2+}$ (**6e**)	(2.617)[d]	(1.0)[d]	(0.06)[d]	
$[Pd_2(dppen)_2(XylNC)_2]^{2+}$ (**6a**)	2.59	1.2	0.065	2.3
$[Pd_2(dppe)_2(XylNC)_2]^{2+}$ (**6b**)	2.60	1.0	0.065	3.1
$[Pd_2(dppp)_2(XylNC)_2]^{2+}$ (**6d**)	2.60	0.8	0.069	7.1
$[Pd_2(dppb)_2(XylNC)_2]^{2+}$ (**6f**)	2.60	0.8	0.062	2.0

[a] The Pd–Pd length, estimated errors are ±0.01 Å. [b] The number of neighboring palladium atoms, estimated errors are ±0.3. [c] $R = \sum|k^3\chi_{dif}(k) - k^3\chi_{calc}(k)|/\sum k^3\chi_{dif}(k)$, where $\chi_{dif}(k)$ and $\chi_{calc}(k)$ are extracted and calculated data, respectively. [d] Reference compound. The values in parentheses were used to determine the parameters of $F_{Pd}(k)$ and $\Phi_{Pd}(k)$.

of the terminal carbon atom of isocyanide, the intense peak at ca. 1.9 Å corresponding to that of the phosphorus atoms of dppp ligands, and the peak at about 2.2 Å attributable to that of the palladium atom, on the basis of the crystal structure. Our attention was focused on the Pd–Pd bond length; however, the peak arising from the Pd atom was overlapped with that from the P atoms, preventing us from obtaining precise structural parameters concerning the metal–metal bond. Thus, the EXAFS analysis was carried out with a modified manner as follows. At first, the set of three peaks was back-Fourier-transformed by a proper window (1.1–2.7 Å), on which the preliminary curve-fitting analysis was performed by means of the three-terms fit, $k^3\chi_{calc}(k) = k^3\chi_C(k) + k^3\chi_P(k) + k^3\chi_{Pd}(k)$, using the theoretical $F_i(k)$ and $\Phi_i(k)$.[29,30] Then, $[k^3\chi_{obsd}(k) - (k^3\chi_C(k) + k^3\chi_P(k))]$ was Fourier transformed to give a difference r spectrum clearly showing the backscattering contribution of the Pd atom (Figure 6b), which was back-Fourier-transformed again by the use of a window (1.8–2.7 Å). The empirical parameters of $F_{Pd}(k)$ and $\Phi_{Pd}(k)$ with respect to the Pd–Pd bond were derived from this extracted EXAFS oscillation for the Pd peak of **6e**.

The analysis of **6a** was carried out in the similar manner (Figure 6c,d), and the extracted EXAFS oscillation for the Pd contribution was subject to curve fitting to give the structural parameters of the Pd–Pd bond (Table VI), which are in good agreement with those from the crystallographic study. The structural parameters of **6b**, **6d**, and **6f** are also summarized in Table VI. In the series of bis(diphosphine) dimers, the Pd–Pd bond lengths fall in a narrow range (2.59–2.62 Å). The coordination numbers (N = 0.8–1.2) are also in accordance with the dimeric structure.

It was revealed that the palladium(I) dimers of diphosphines (**6**) have quite long Pd–Pd bonds, and their distances are not influenced by the carbon chain of diphosphine ligands. Since the high reactivity of such a long metal–metal bond is readily predicted, we are now examining the insertion reactions of small molecules and ML_2 fragments into the metal–metal bond and the homolytic cleavage reactions.

Acknowledgment. This work was partially supported by a Grant-in-Aid for Scientific Research from the Ministry of Education of Japan, and a grant from Futaba Denshi-kogyo.

Supplementary Material Available: Listings of crystallographic data, positional and anisotropic thermal parameters, atomic parameters of hydrogen atoms, and bond distances and angles for **5b**, **6a**, and **6e** and figures showing the results of curve fitting analyses for the Pd–Pd contribution in **6a**, **6b**, **6d**, **6e**, and **6f** (32 pages). Ordering information is given on any current masthead page.